Brain Advance Access published July 25, 2015

doi:10.1093/brain/awv219 BRAIN 2015: Page 1 of 13 | 1

BRAIN
A JOURNAL OF NEUROLOGY

Loss of phosphodiesterase 10A expression is associated with progression and severity in Parkinson's disease

Flavia Niccolini,[1,2] Thomas Foltynie,[3] Tiago Reis Marques,[4] Nils Muhlert,[5,6] Andri C. Tziortzi,[7] Graham E. Searle,[7] Sridhar Natesan,[4] Shitij Kapur,[4] Eugenii A. Rabiner,[7,8] Roger N. Gunn,[2,7] Paola Piccini[2] and Marios Politis[1,2]

The mechanisms underlying neurodegeneration and loss of dopaminergic signalling in Parkinson's disease are still only partially understood. Phosphodiesterase 10A (PDE10A) is a basal ganglia expressed dual substrate enzyme, which regulates cAMP and cGMP signalling cascades, thus having a key role in the regulation of dopaminergic signalling in striatal pathways, and in promoting neuronal survival. This study aimed to assess *in vivo* the availability of PDE10A in patients with Parkinson's disease using positron emission tomography molecular imaging with ^{11}C-IMA107, a highly selective PDE10A radioligand. We studied 24 patients with levodopa-treated, moderate to advanced Parkinson's disease. Their positron emission tomography imaging data were compared to those from a group of 12 healthy controls. Parametric images of ^{11}C-IMA107 binding potential relative to non-displaceable binding (BP_{ND}) were generated from the dynamic ^{11}C-IMA107 scans using the simplified reference tissue model with the cerebellum as the reference tissue. Corresponding region of interest analysis showed lower mean ^{11}C-IMA107 BP_{ND} in the caudate ($P < 0.001$), putamen ($P < 0.001$) and globus pallidus ($P = 0.025$) in patients with Parkinson's disease compared to healthy controls, which was confirmed with voxel-based analysis. Longer Parkinson's duration correlated with lower ^{11}C-IMA107 BP_{ND} in the caudate ($r = -0.65$; $P = 0.005$), putamen ($r = -0.51$; $P = 0.025$), and globus pallidus ($r = -0.47$; $P = 0.030$). Higher Unified Parkinson's Disease Rating Scale part-III motor scores correlated with lower ^{11}C-IMA107 BP_{ND} in the caudate ($r = -0.54$; $P = 0.011$), putamen ($r = -0.48$; $P = 0.022$), and globus pallidus ($r = -0.70$; $P < 0.001$). Higher Unified Dyskinesia Rating Scale scores in those Parkinson's disease with levodopa-induced dyskinesias ($n = 12$), correlated with lower ^{11}C-IMA107 BP_{ND} in the caudate ($r = -0.73$; $P = 0.031$) and putamen ($r = -0.74$; $P = 0.031$). Our findings demonstrate striatal and pallidal loss of PDE10A expression, which is associated with Parkinson's duration and severity of motor symptoms and complications. PDE10A is an enzyme that could be targeted with novel pharmacotherapy, and this may help improve dopaminergic signalling and striatal output, and therefore alleviate symptoms and complications of Parkinson's disease.

1 Neurodegeneration Imaging Group, Department of Basic and Clinical Neuroscience, Institute of Psychiatry, Psychology and Neuroscience, King's College London, London, UK
2 Division of Brain Sciences, Department of Medicine, Imperial College London, London, UK
3 Sobell Department of Motor Neuroscience, UCL Institute of Neurology, London, UK
4 Department of Psychosis Studies, Institute of Psychiatry, Psychology and Neuroscience, King's College London, London, UK
5 School of Psychology and Cardiff University Brain Research Imaging Centre, Cardiff University, UK
6 School of Psychological Sciences, University of Manchester, Manchester, UK
7 Imanova Ltd., Centre for Imaging Sciences, Hammersmith Hospital, London, UK
8 Department of Neuroimaging, Institute of Psychiatry, Psychology and Neuroscience, King's College London, London, UK

Correspondence to: Marios Politis,
Neurodegeneration Imaging Group,
Maurice Wohl Clinical Neuroscience Institute,

Received April 1, 2015. Revised May 24, 2015. Accepted June 13, 2015.

125 Coldharbour Lane, Camberwell,
London SE5 9NU, UK
E-mail: marios.politis@kcl.ac.uk

Keywords: Parkinson's disease; PDE10A; PET; motor; LIDs

Abbreviations: BP_{ND} = non-displaceable binding potential; LIDs = levodopa-induced dyskinesias; UDysRS = Unified Dyskinesia Rating Scale; UPDRS = Unified Parkinson's Disease Rating Scale

Introduction

Parkinson's disease is a chronic and progressive neurodegenerative disorder characterized by the loss of dopaminergic neurotransmission in the denervated areas of the forebrain, above all in the striatum (Jellinger, 1991). The mechanisms underlying the progressive loss of dopamine neuron function and the development of motor symptoms and complications are still only partially understood. Dopamine replacement therapy such as with levodopa, remains the gold standard of therapy, several decades since the original work by Cotzias and colleagues (1967, 1969). Although levodopa has been a remarkable success in Parkinson's therapeutics, it has not delivered a complete solution for the patients. Following years of exposure, levodopa loses its efficacy and patients develop motor complications such as levodopa-induced dyskinesias (LIDs) (Lees *et al.*, 1977). There is an urgent need for complementary and alternative treatments and currently no treatment has been proven useful slowing down the progression of Parkinson's disease or for managing LIDs effectively.

Phosphodiesterase 10A (encoded by *PDE10A*) is a dual substrate enzyme located almost exclusively within the basal ganglia and mainly in the axons of the striatal medium spiny neurons, where it hydrolyses cAMP and cGMP (Fujishige *et al.*, 1999; Coskran *et al.*, 2006). In the striatal pathway, PDE10A regulates cAMP/cGMP downstream signalling cascades (e.g. cAMP/PKA/DARPP-32) that control a diverse array of neural functions ranging from ion conductance to synaptic plasticity playing a key role in the regulation of dopaminergic signalling in the direct and indirect striatal pathways (Nishi *et al.*, 2008; Girault, 2012).

Preclinical studies in levodopa naïve animal models of Parkinson's disease have shown that unilateral lesion of nigrostriatal dopaminergic projections leads to increased cAMP levels in the ipsilateral striatum compared to the contralateral non-lesioned side (Hossain and Weiner, 1993; Tenn and Niles, 1997; Giorgi *et al.*, 2008). In striatal neurons, cAMP synthesis is regulated by dopamine through the interaction with D1 and D2 receptors and its catabolism is mediated by phosphodiesterases such as PDE10A (Rasmussen, 1970). In animal models of Parkinson's disease, unilateral lesion of nigrostriatal projections not only induces an increase of cAMP but also downregulates PDE10A mRNA and protein levels in the striatum and globus pallidus compared to the contralateral non-lesioned side (Giorgi *et al.*, 2008, 2011). These data demonstrated that lesions of the midbrain dopaminergic neurons could regulate both PDE10A expression and the rate of cAMP catabolism in the basal ganglia. The PDE10A/cAMP interaction is essential for dopamine neurotransmission and could have a key role in the pathophysiology of Parkinson's disease. Moreover, cyclic nucleotides levels were reduced at peak dyskinesias in rodent models of Parkinson's disease and administration of phosphodiesterase inhibitors before levodopa decreased the severity of dyskinesias (Giorgi *et al.*, 2008; Sancesario *et al.*, 2014).

Here, we investigated *in vivo* the expression of PDE10A in patients with Parkinson's disease, using PET with ^{11}C-IMA107, which is a specific and highly potent PDE10A radioligand for human use (Plisson *et al.*, 2014). Our findings suggest loss of striatal and pallidal PDE10A expression in patients with Parkinson's disease, which is associated with progression of the disease and severity of motor signs and complications.

Materials and methods

Participants and clinical characteristics

Twenty-four patients with idiopathic Parkinson's disease according to the UK Brain Bank criteria (12 of whom had a history of levodopa related motor complications, 12 with a stable levodopa motor response) were recruited from specialist Movement Disorders clinics at Imperial College Healthcare NHS Trust and National Hospital of Neurology and Neurosurgery, Queen Square, London (Table 1). Twelve healthy individuals (mean age ± SD: 51.1 ± 11.1 years) with no history of neurological or psychiatric disorders, served as the control group. All participants screened successfully to undertake PET and MRI scanning under standard criteria (http://www.mrisafety.com; https://www.gov.uk/government/publications/arsac-notes-for-guidance), had no history of other neurological or psychiatric disorders, and were not under treatment with substances with known actions in phosphodiesterases (e.g. aminophylline, paraxanthine, theobromine, ibudilast and papaverine).

Patients with Parkinson's disease were on levodopa treatment for at least 6 months at the time of study enrolment. Daily dopaminergic medication dose was calculated with a formula based on the theoretical equivalence to levodopa (Politis *et al.*, 2010; Supplementary material). Motor symptom severity was assessed with the Unified Parkinson's Disease

Table 1 Clinical characteristics of Parkinson's disease patients

Subject	Sex	Age (years)	Disease duration[a]	Parkinson's disease medication duration (years)	Daily LED (mg)	Hoehn and Yahr OFF	Hoehn and Yahr ON	UPDRS-III OFF[e]	UPDRS-III ON	UPDRS-IV	UDysRS	PDQ-39
1	M	69.6	12	11	1377	4	4	68	38	11	81	49
2	F	78.5	24	20	1329	4	4	71	54	17	109	30
3	M	66.1	14	13	2662.5	4	2	54	19	17	94	49
4	F	56.2	12	11	1715	2	2	46	16	1	98	33
5	F	59.0	13	12	973	4	3	61	11	11	55	49
6	M	59.9	9	8	520	2.5	2	29	9	5	86	16
7	M	56.8	12	10	2937	3	2	33	10	12	102	56
8	F	70.1	12	10	946	3	1.5	20	11	13	80	45
9	M	72.5	16	12	2873.75	4	3	64	13	17	114	35
10	M	69.4	9	8	1874.5	2	1	35	8	9	99	44
11	F	53.1	17	14	697	2	2	53	4	10	126	43
12	M	72.4	8	6	452	3	3	32	15	12	82	56
13	M	72.0	8	8	640	2	2	34	14	0	0	41
14	M	71.8	8	7	1515	2	2	48	36	0	0	36
15	F	67.4	5	0.9	400	1	1	10	2	0	0	22
16	F	71.3	5	3	850	2	1	35	6	0	0	45
17	M	75.5	4	3	300	2	1	21	5	0	0	7
18	F	57.2	1	10	150	1	0	6	0	0	0	7
19	M	72.9	11	9	960	2	1	39	15	0	0	7
20	F	71.3	5	5	510	1.5	1.5	11	6	0	0	62
21	F	59.8	7	6	480	1.5	1	27	6	0	0	10
22	F	62.2	4	3	920	2	1	30	11	0	0	72
23	M	70.5	8	5	490	2	1	19	8	0	0	6
24	M	75.5	8	6	1336.25	2	1	23	13	0	0	15
AVG (±SD)[b]	13M/11F	67.13 (±7.2)	9.67 (±5.0)	8.37 (±4.3)	1121.17 (±799.0)	2.44 (±1.0)	1.79 (±1.0)	36.21 (±18.5)	13.75 (±12.4)	5.63 (±6.6)[b]	46.92 (±49.6)[b]	34.79 (±19.5)

[a]From time of first appearance of Parkinson's disease motor symptoms;.
[b]AVG (±SD) of 12 Parkinson's disease patients with LIDs.
LED = levodopa equivalent dose; PDQ-39 = 39-item Parkinson's Disease Questionnaire.

Rating Scale part-III (UPDRS-III) and staged with Hoehn and Yahr scale. For correlation with the PET data, we divided UPDRS-III in tremor, rigidity, bradykinesia and axial subscores (Supplementary material). Presence/absence of motor complications was assessed with the UPDRS part-IV (UPDRS-IV). Severity of LIDs was assessed with the Unified Dyskinesia Rating Scale (UDysRS). Motor assessments were performed OFF medication after overnight withdrawal of patient's dopaminergic medications, and also following a challenge with levodopa 250/carbidopa 25, with an observational ON-medication period of 150 min. Quality of life was measured with the patient self-reported 39-item Parkinson's disease Questionnaire (PDQ-39).

The study was approved by the institutional review boards and the research ethics committee. Written informed consent was obtained from all study participants in accordance with the Declaration of Helsinki.

Scanning procedures

PET and MRI were performed at Imanova Ltd, London, UK. All participants were scanned on Siemens Biograph Hi-Rez 6 PET-CT scanner, 1 h after a standard levodopa 250/carbidopa 25 dose. A mean dose of 289 MBq ^{11}C-IMA107 (SD: ± 39.2) [mean mass injected: 3.5 μg (SD: ± 1.8)] was administered intravenously as a slow bolus injection over 20 s. All participants were scanned after withholding consumption of caffeinated beverages for 12 h (Fredholm *et al.*, 1999).

Dynamic emission data were acquired continuously for 90 min after the injection of ^{11}C-IMA107. The dynamic images were reconstructed into 26 frames (8 × 15 s, 3 × 60 s, 5 × 120 s, 5 × 300 s, and 5 × 600 s), using a filtered back projection algorithm (direct inversion Fourier transform) with a 128 matrix, zoom of 2.6 producing images with isotropic voxel size of 2 × 2 × 2 mm^3, and smoothed with a transaxial Gaussian filter of 5 mm.

MRI scans were acquired with a 32-channel head coil on a Siemens Magnetom Verio, 3 T MRI scanner and included a T_1-weighted magnetization prepared rapid gradient echo sequence (MPRAGE; time repetition = 2300 ms, time echo = 2.98 ms, flip angle of 9°, time to inversion = 900 ms, matrix = 240 × 256); fast grey matter T_1 inversion recovery (FGATIR; repetition time = 3000 ms, echo time = 2.96 ms, flip angle of 8°, time to inversion = 409 ms, matrix = 240 × 256) (Sudhyadhom *et al.*, 2009) and fluid and white matter suppression (FLAWS; repetition time = 5000 ms, echo time = 2.94 ms, flip angle of 5°, time to inversion = 409/1100 ms, matrix = 240 × 256) (Tanner *et al.*, 2013) sequences for co-registration with the PET images and for improving delineation of subcortical brain regions. All sequences used a 1 mm^3 voxel

size, anteroposterior phase encoding direction, and a symmetric echo.

Imaging data analysis

MRI-based volumetric analysis

Because PDE10A is an intracellular enzyme mainly expressed in the basal ganglia nuclei (Fujishige *et al.*, 1999; Coskran *et al.*, 2006), degeneration of these nuclei may affect the expression of the enzyme. Thus, we investigated volumetric changes in basal ganglia nuclei and thalamus in our cohort of Parkinson's disease patients. We used the FreeSurfer's image analysis suite (version 5.3.0 http://surfer.nmr.mgh.harvard.edu) to process individual MRI scans for deriving measures of cortical and subcortical volumes. The automated procedures for acquiring volumetric measures of brain structures have been previously described (Fischl *et al.*, 2002). This procedure automatically assigns a neuroanatomical label to each voxel in an MRI volume based on probabilistic information automatically estimated from a manually labelled training set. In brief, the segmentation is carried out as follows: first, an optimal linear transform is computed that maximizes the likelihood of the input image, given an atlas constructed from manually labelled images. Then, a non-linear transform is initialized with the linear one, and the image is allowed to further deform to better match the atlas. Finally, a Bayesian segmentation procedure is carried out, and the maximum *a posteriori* estimate of the labelling is computed. The segmentation uses three pieces of information to disambiguate labels: (i) the prior probability of a given tissue class occurring at a specific atlas location; (ii) the likelihood of the image intensity given that tissue class; and (iii) the probability of the local spatial configuration of labels given the tissue class. This technique has previously been shown to be comparable in accuracy to manual labelling (Fischl *et al.*, 2002). Adjustments for intracranial volume were calculated for each region of interest using validated methods within the FreeSurfer toolkit (Buckner *et al.*, 2004).

^{11}C-IMA107 PET data analysis

Movement correction

Subjects were positioned supine with their transaxial planes parallel to the line intersecting the anterior-posterior commissure line. Head position was maintained with the help of individualized foam holders, monitored by video and was repositioned if movement was detected. Subjects were in a resting state with low light. Intrascan notes for participant's movement were acquired during scanning. We applied correction for movement using a frame-by-frame realignment procedure as previously described (Montgomery *et al.*, 2006) with in-house software (c-wave) implemented in Matlab 8.2 (The MathWorks Inc.). Attenuated corrected images were realigned using a mutual information algorithm (Studholme *et al.*, 1997) excluding the first seven frames containing little information. Frame 17 was chosen as the reference frame because it offered good signal-to-noise ratio. Frames 8–26 of the original time series were then resliced and reassembled into a movement-corrected dynamic scan. Decay-corrected time–activity curves were derived and compared to those without movement correction. Amount and timing of any movement were assessed graphically and compared with intrascan notes.

Parametric images

First, integrated (ADD) images were created by summing the time series of ^{11}C-IMA107 uptake scans collected 0–90 min after tracer administration. Then, parametric images of ^{11}C-IMA107 non-displaceable binding potential (BP_{ND}) were generated using a basis function implementation of the simplified reference tissue model, with the cerebellum as the reference tissue for non-specific binding using an in-house software (c-wave) implemented in Matlab 8.2 (Gunn *et al.*, 1997). Previous PET studies have shown lower PDE10A uptake in the cerebellum (Plisson *et al.*, 2011, 2014; Barret *et al.*, 2014) and a blocking study with selective PDE10A inhibitors has shown no changes in cerebellar ^{11}C-IMA107 binding (Imanova internal data), confirming the suitability of the cerebellum as a reference region for the determination of the regional estimation of BP_{ND}.

Region of interest-based analysis

To facilitate anatomical delineation of regions of interest, PET images were anatomically co-registered and resliced to the corresponding volumetric FLAWS and FGATIR magnetic resonance images and spatially normalized into the T_1-weighted MNI 152 template using the Mutual Information Registration algorithm in Statistical Parametric Mapping version 8 (SPM8) software package implemented in Matlab 8.2. Regions of interest were delineated manually on the co-registered MRIs using ANALYZE version 11 (Mayo Foundation) medical imaging software package by the assessor who was blinded to groups allocation. We manually delineated basal ganglia structures due to the modest performance of automated parcellation techniques on structures such as the substantia nigra, which have poor contrast on structural T_1-weighted magnetic resonance images. To compensate for this, we acquired state-of-the-art FGATIR and FLAWS MRI sequences for each individual, which use T_1-nulling to minimize white matter signal and, by improving contrast, increase the definition of basal ganglia structures. We have then used a reliable, robust and repeatable technique for manual delineation of basal ganglia structures (Tziortzi *et al.*, 2011). This technique has shown low BP_{ND} variability for both the intra- and inter-operator comparisons and good level of agreement with automatically derived regions of interest (Tziortzi *et al.*, 2011). Regions of interest included caudate, putamen, ventral striatum, globus pallidus (external and internal segment), substantia nigra and motor thalamic nuclei. These brain regions express PDE10A to a varying degree (Seeger *et al.*, 2003; Coskran *et al.*, 2006).

Voxel-based analysis

Spatial preprocessing and statistical analyses were performed using SPM8 implemented in Matlab 8.2. First, ADD images were co-registered to the corresponding T_1-weighted magnetic resonance images using a normalized mutual-information-based six parameter rigid registration. The resulting transformation matrix was then applied to the corresponding ^{11}C-IMA107 BP_{ND} images. Then, T_1-weighted magnetic resonance images were spatially normalized to the T_1 MNI template provided with SPM8 (Ashburner and Friston, 1999). The transformation parameters obtained were then applied to the co-registered BP_{ND} images. Parametric images were

spatially smoothed using an 8 mm full-width at half-maximum Gaussian kernel. This spatial filter accommodates interindividual anatomic variability and improves signal to noise for the statistical analysis. Voxel-wise statistics for between-group comparisons were computed using appropriately weighted contrasts to localize significant decreases in mean voxel ^{11}C-IMA107 BP_{ND} values after applying the Basal Ganglia Human Area Template (Prodoehl *et al.*, 2008). The contrasts were used to derive Z-scores on a voxel basis using the general linear model (Friston *et al.*, 1995). The threshold for statistical significance was set to $P < 0.05$ after family wise error (FWE) correction for multiple comparisons.

Statistical analysis

Statistical analysis and graph illustration were performed with SPSS (version 20) and GraphPad Prism (version 6.0c) for MAC OS X, respectively. For all variables, variance homogeneity and Gaussianity were tested with Bartlett and Kolmogorov-Smirnov tests and we proceeded with parametric tests as our PET and clinical data were normally distributed. Multivariate analysis of variance (MANOVA) was used to assess the main effects of regional ^{11}C-IMA107 BP_{ND} between patients with Parkinson's disease and healthy controls. If the overall multivariate test was significant, *P*-values for each variable were calculated following Bonferroni's multiple-comparisons test. We interrogated correlations between PET and clinical data using Pearson *r* and we applied the Benjamini-Hochberg correction to reduce false discovery rate (Benjamini and Hochberg, 1995). We set the false discovery rate cut-off at 0.05. Partial correlation analysis was performed to control for the effect of disease duration on UDysRS score/^{11}C-IMA107 BP_{ND} correlation. All data are presented as mean ± standard deviation (SD), and the level α was set for all comparisons at $P < 0.05$, corrected. In addition, we performed SPM voxel-by-voxel comparison between controls and Parkinson's disease patients. These comparisons were based on *a priori* hypothesis restricted to a volume of interest, which included the basal ganglia in both hemispheres (Prodoehl *et al.*, 2008). This masking drastically reduces the number of voxel-by-voxel statistical comparisons, and a cluster-corrected threshold of $P < 0.05$ used to test for statistically significant effects. Striatal ^{11}C-IMA107 BP_{ND} results were corrected for multiple comparisons using Gaussian random field theory. As no changes were found within the pallidum at this level, for completeness changes in pallidal PDE10A expression were investigated using a more liberal threshold of $P < 0.05$ (extent threshold of 10 voxels), to rule out the risk of a type II error (false negative).

Results

Volumetric analysis

Freesurfer analysis showed no volumetric differences in left and right basal ganglia and thalamic regions of interest between the groups of Parkinson's disease patients and healthy controls (Supplementary Table 1).

Region of interest-based analysis

We found significant differences in mean ^{11}C-IMA107 BP_{ND} between Parkinson's disease patients and healthy controls ($P < 0.001$; Table 2, Fig. 1 and Supplementary Fig. 1). Patients with Parkinson's disease had significantly lower mean ^{11}C-IMA107 BP_{ND} in caudate ($P < 0.001$; −28.4%), putamen ($P < 0.001$; −25.5%) and globus pallidus ($P = 0.025$; −14.2%) compared to healthy controls. Within the globus pallidus, loss of ^{11}C-IMA107 BP_{ND} was driven by the internal segment ($P = 0.018$; −18.8%). There were no differences in ^{11}C-IMA107 BP_{ND} between the patients with Parkinson's disease and healthy controls in ventral striatum ($P > 0.10$; −1.6%), substantia nigra ($P > 0.10$; −12.4%) and motor thalamic nuclei ($P > 0.10$; −12.3%).

We assessed whether clinically asymmetric limb motor features correspond to ^{11}C-IMA107 BP_{ND} decreases, and we found no significant differences in ^{11}C-IMA107 BP_{ND} between the most and less affected sides ($P = 0.43$; Supplementary Table 2). Moreover, we found no effect of age in ^{11}C-IMA107 BP_{ND} in all the regions examined in the group of healthy controls ($P = 0.32$).

The 24 patients with Parkinson's disease were further divided into two subgroups, depending on whether they were stable responders to levodopa ($n = 12$) or had LIDs ($n = 12$). We found significant differences in mean ^{11}C-IMA107 BP_{ND} between Parkinson's disease patients with stable levodopa response and those with LIDs ($P = 0.002$; Table 3). Parkinson's disease patients with LIDs had significantly lower mean ^{11}C-IMA107 BP_{ND} in caudate ($P = 0.045$; −18.60%), substantia nigra ($P < 0.001$; −33.50%) and motor thalamic nuclei ($P = 0.009$; −29.3%) compared to stable levodopa responders. Parkinson's disease patients with LIDs had longer disease duration than patients with Parkinson's disease who were stable responders to levodopa (6.16 ± 2.6 versus 13.17 ± 4.3 years; $P < 0.001$). After controlling for disease duration, we did not find significant differences in ^{11}C-IMA107 BP_{ND} between Parkinson's disease patients with stable levodopa response and those with LIDs ($P > 0.05$).

Voxel-based analysis

Voxel-by-voxel analysis of ^{11}C-IMA107 parametric images between the group of Parkinson's disease patients and healthy controls confirmed results obtained with region of interest analysis. SPM analysis within the basal ganglia mask localized clusters of significant decreases in the right and left caudate ($P < 0.05$ corrected), putamen ($P < 0.05$ corrected) and globus pallidus ($P < 0.05$ uncorrected) in the Parkinson's disease patients when compared with the group of healthy controls (Table 4 and Fig. 2). We repeated the SPM analysis using LED as a covariate and the results remained significant. We did not find any differences in ^{11}C-IMA107 BP_{ND} at a voxel-level between the

Table 2 ^{11}C-IMA107 BP_{ND} in the groups of Parkinson's disease patients and healthy controls.

Anatomical region of interest	Healthy controls (mean ± SD)	Parkinson's disease (mean ± SD)	*P*-value*	% change in Parkinson's disease
Striatum	1.81 (±0.28)	1.40 (±0.23)	**<0.001**	**−22.8%**
Caudate	1.37 (±0.25)	0.98 (±0.18)	**<0.001**	**−28.4%**
Putamen	2.21 (±0.31)	1.64 (±0.29)	**<0.001**	**−25.5%**
Ventral striatum	1.16 (±0.24)	1.14 (±0.22)	>0.10	−1.6%
Globus pallidus	1.75 (±0.33)	1.50 (±0.24)	**0.025**	**−14.3%**
Globus pallidus external	1.91 (±0.39)	1.72 (±0.25)	>0.10	−9.6%
Globus pallidus internal	1.54 (±0.27)	1.25 (±0.23)	**0.018**	**−18.8%**
Substantia nigra	0.49 (±0.12)	0.55 (±0.17)	>0.10	+ 12.4%
Motor thalamic nuclei	0.45 (±0.07)	0.39 (±0.11)	>0.10	−12.3%

*P-values are Bonferroni corrected. Significant *P*-values and per cent changes are highlighted in bold.

Parkinson's disease patients with stable levodopa response and those with LIDs.

Correlations

Disease severity

Longer Parkinson's disease duration correlated with lower ^{11}C-IMA107 BP_{ND} in caudate ($r = -0.65$; $P = 0.005$), putamen ($r = -0.51$; $P = 0.025$) and globus pallidus ($r = -0.47$; $P = 0.03$; Fig. 3A). Higher UPDRS-III motor scores (corrected for disease duration) were also correlated with lower ^{11}C-IMA107 BP_{ND} in the caudate ($r = -0.54$; $P = 0.011$), putamen ($r = -0.48$; $P = 0.022$) and globus pallidus ($r = -0.70$; $P < 0.001$; Fig. 3B).

With regards to UPDRS-III subscores (corrected for disease duration), higher bradykinesia subscores correlated with lower ^{11}C-IMA107 BP_{ND} in the caudate ($r = -0.58$; $P = 0.007$), putamen ($r = -0.53$; $P = 0.010$) and globus pallidus ($r = -0.69$; $P < 0.001$; Fig. 3C). Higher rigidity correlated with lower ^{11}C-IMA107 BP_{ND} in the caudate ($r = -0.51$; $P = 0.022$), putamen ($r = -0.48$; $P = 0.022$) and globus pallidus ($r = -0.67$; $P < 0.001$; Fig. 3D). Higher axial subscores correlated only with lower ^{11}C-IMA107 BP_{ND} in the globus pallidus ($r = -0.57$; $P = 0.009$; Supplementary Fig. 2). We did not find any correlations between tremor subscores, Hoehn and Yahr staging scores, PDQ-39 ratings and PDE10A data.

Motor complications

Higher UDysRS scores correlated with lower ^{11}C-IMA107 BP_{ND} in the caudate ($r = -0.73$, $P = 0.031$) and putamen ($r = -0.74$, $P = 0.031$; Fig. 4). After controlling for disease duration, the correlation remained significant between higher UDysRS scores and lower ^{11}C-IMA107 BP_{ND} in the caudate ($r = -0.66$, $P = 0.027$) and putamen ($r = -0.68$, $P = 0.022$).

Dopaminergic medication

We found a significant interaction between higher daily LED and longer disease duration ($r = 0.52$; $P = 0.014$), higher UPDRS-III scores ($r = 0.055$; $P = 0.012$), and lower ^{11}C-IMA107 BP_{ND} in the regions of interest examined ($r = -0.44$; $P = 0.036$). Subsequently, we repeated the PET-clinical correlation analysis adding LED as a covariate and found no changes in the level of significance of the previously reported correlations between lower ^{11}C-IMA107 BP_{ND} and (i) longer disease duration ($r = -0.55$; $P = 0.020$); and (ii) higher UPDRS-III motor scores ($r = -0.64$; $P = 0.008$).

Discussion

Our findings indicate loss of PDE10A signalling in the striatum and globus pallidus of patients with Parkinson's disease, which is associated with the duration of the disease and the severity of motor signs and complications such as LIDs. Our findings are consistent with preclinical data showing that lesion of dopaminergic neurons induces significant decreases in striatal and pallidal PDE10A mRNA and protein levels (Giorgi *et al.*, 2011; Sancesario *et al.*, 2014), and suggest that nigrostriatal degeneration affects the expression of PDE10A.

Our region of interest analysis demonstrated 14–28% significant loss of striatal and pallidal PDE10A expression in patients with moderate to advanced Parkinson's disease who had mean disease duration of 9.7 years, were on dopamine-replacement therapy, and had no significant brain atrophy in the regions of interest examined. We confirmed these results at a voxel level. Although Parkinson's disease patients were older than the group of healthy controls, we did not find any effect of age in PDE10A expression in the regions of interest examined. This observation is in line with recent experimental work, which indicates no significant effect of age in striatal PDE10A mRNA and protein levels in mice (Kelly *et al.*, 2014).

There were strong associations between loss of striatal and pallidal PDE10A expression and Parkinson's duration and severity of motor symptoms. We found correlations between loss of striatal and pallidal PDE10A expression, longer disease duration and worse motor symptoms as assessed by UPDRS-III. The motor symptoms that were

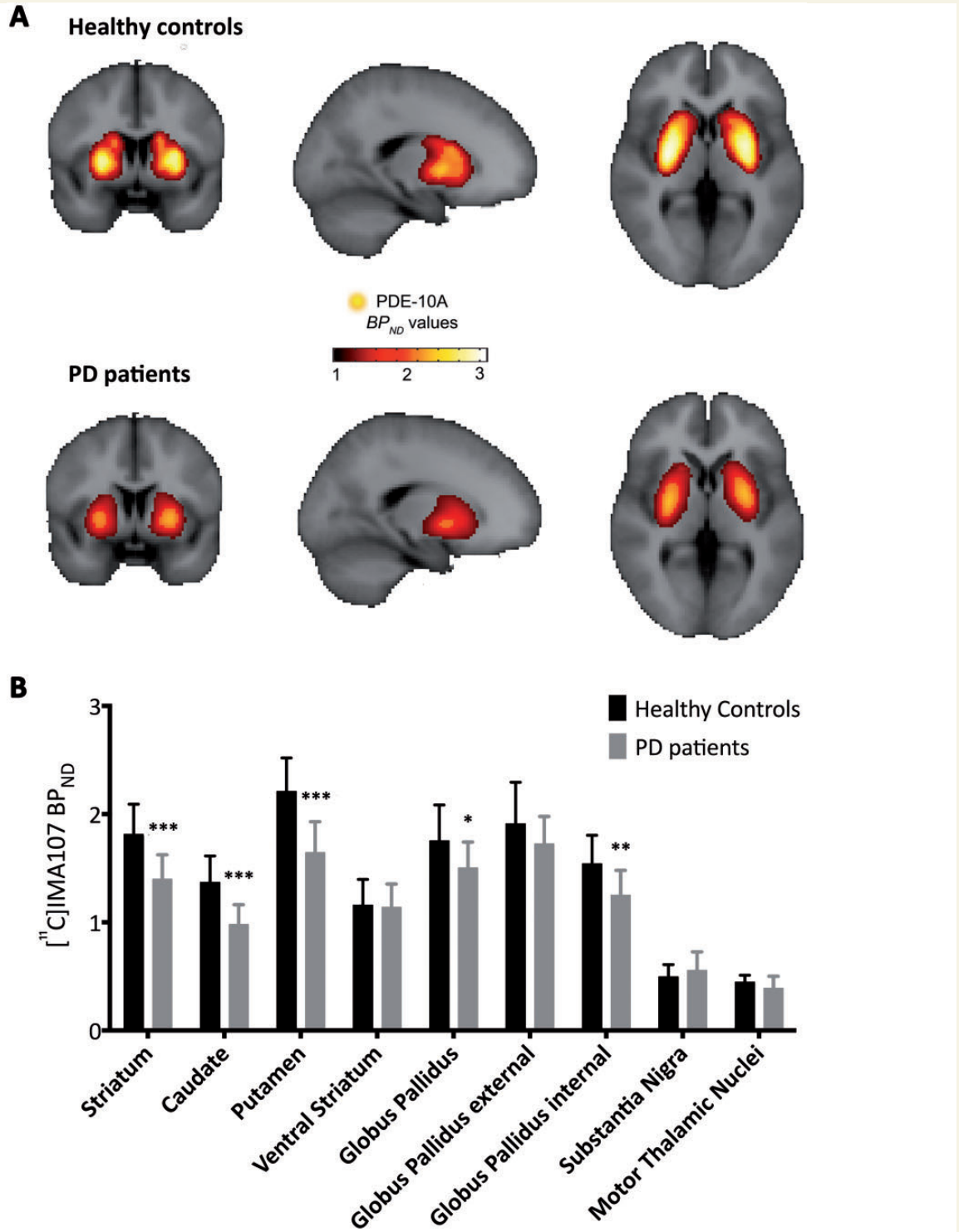

Figure 1 Altered PDE10A expression in manually defined brain regions of Parkinson's disease patients. (**A**) Mean ^{11}C-IMA107 BP_{ND} parametric images derived from 12 healthy controls and 24 patients with Parkinson's disease (PD) in stereotaxic space overlaid onto the T_1-weighted MNI template showing significant loss of striatal and pallidal PDE10A signal in the Parkinson's disease patients. (**B**) Bar graph showing mean ^{11}C-IMA107 BP_{ND} in anatomically defined brain regions between Parkinson's disease patients and healthy controls. Colour bar reflects range of ^{11}C-IMA107 BP_{ND} intensity. Error bars represent mean ± SD. *$P < 0.05$; **$P < 0.01$; ***$P < 0.001$.

Table 3 ^{11}C-IMA107 BP_{ND} in the groups of Parkinson's disease patients with levodopa-induced dyskinesias and stable response to levodopa

Anatomical regions of interest	Parkinson's disease stable (n = 12) (mean ± SD)	Parkinson's disease LIDs (n = 12) (mean ± SD)	P-value*	% change in Parkinson's disease LIDs
Striatum	1.48 (±0.24)	1.31 (±0.18)	>0.10	−11.7%
Caudate	1.08 (±0.19)	0.88 (±0.10)	**0.045**	**−18.6%**
Putamen	1.74 (±0.31)	1.55 (±0.23)	>0.10	−10.9%
Ventral striatum	1.23 (±0.21)	1.04 (±0.19)	>0.10	−15.4%
Globus pallidus	1.60 (±0.24)	1.40 (±0.21)	>0.10	−12.4%
Globus pallidus external	1.82 (±0.24)	1.63 (±0.23)	>0.10	−10.8%
Globus pallidus internal	1.35 (±0.24)	1.15 (±0.17)	>0.10	−15.0%
Substantia nigra	0.67 (±0.15)	0.44 (±0.11)	**<0.001**	**−33.5%**
Motor thalamic nuclei	0.46 (±0.11)	0.32 (±0.07)	**0.009**	**−29.3%**

*P-values are Bonferroni corrected but are not corrected for disease duration. Statistical significance was lost after using disease duration as a covariate in the analysis. Significant P-values and per cent changes are highlighted in bold.

driving this correlation were bradykinesia and rigidity, whereas worse axial symptoms correlated with decreased PDE10A expression only in globus pallidus. Loss of PDE10A expression was not associated with tremor signs.

PET and SPECT studies with dopaminergic markers have shown correlations between dopaminergic decline, Parkinson's progression and worse clinical severity (Otsuka *et al.*, 1996; Booij *et al.*, 1997; Broussolle *et al.*, 1999; Marek *et al.*, 2001; Hsiao *et al.*, 2014). A previous study has reported correlations between striatal decreases in ^{18}F-DOPA uptake and longer disease duration and worse UPDRS-III motor scores at a 0.01 and 0.05 α level, respectively (Broussolle *et al.*, 1999). ^{18}F-DOPA and ^{18}F-DTBZ PET studies have shown correlations between dopaminergic decline, worse bradykinesia and rigidity, but not tremor scores in groups of 17–27 patients with Parkinson's disease (Otsuka *et al.*, 1996; Broussolle *et al.*, 1999). In our study, decreased PDE10A expression correlated with longer Parkinson's disease duration and worse severity of bradykinesia and rigidity, at a similar level of statistical significance to that previously seen with dopaminergic imaging markers.

Although previous PET and SPECT studies have predominantly reported correlations between decreases in putaminal dopaminergic markers and Parkinson's motor symptoms (Otsuka *et al.*, 1996; Broussolle *et al.*, 1999), here we found that also caudate PDE10A decreases were associated with worse clinical scores. Our findings are consistent with a minority of previous dopaminergic PET and SPECT studies, which have shown correlations between lower caudate VMAT-2 (encoded by *SLC18A2*) and dopamine transporter (DAT, encoded by *SLC6A3*) levels and worse clinical scores (Marek *et al.*, 2001; Hsiao *et al.*, 2014), and therefore provide support for the role of caudate in the development of motor symptoms in Parkinson's disease.

A striking feature of nigrostriatal dopaminergic degeneration in idiopathic Parkinson's disease is the clinically asymmetric presentation. We assessed whether clinically asymmetric limb motor features correspond to PDE10A decreases, and we found no significant differences in PDE10A expression between most and least affected sides in our cohort of Parkinson's disease patients. It is possible that loss of PDE10A expression does not follow the pattern of dopaminergic degeneration; however, we speculate that this result could be due to the fact that the vast majority of the Parkinson's patients had bilateral disease, all Parkinson's patients were on levodopa therapy and had their PET scans while ON levodopa medication. A recent experimental study has demonstrated that levodopa treatment reduced PDE10A levels in the unlesioned striatum of 6-hydroxydopamine (6-OHDA) lesioned animals (Sancesario *et al.*, 2014). In humans, it would be interesting to investigate the relationship between clinically asymmetric motor features and PDE10A expression in early *de novo* Parkinson's patients in a future study.

Our results also suggest that exogenous dopaminergic medication could have a degree of influence in striatal PDE10A expression in patients with Parkinson's disease. However, covariate analysis indicated that this influence was weak and it did not alter the results of our study. It is important to note that the vast majority of our cohort of Parkinson's patients had established disease and significant motor symptoms with bilateral presentation. Experimental studies have shown that levodopa treatment balances PDE10A levels by reducing PDE10A expression in the unlesioned striatum, without significantly affecting the PDE10A expression in the lesioned striatum of 6-OHDA animals (Sancesario *et al.*, 2014). We believe that chronic effect of levodopa could be investigated by studying in parallel a cohort of unilaterally affected *de novo* Parkinson's patients, whereas the acute levodopa effect could be better understood if OFF and ON levodopa PDE10A PET scans are performed and compared in the same patients with Parkinson's disease.

Table 4 Voxel-based analysis: bilateral striatal significant decreases in ^{11}C-IMA107 BP_{ND} in Parkinson's patients compared with the group of healthy controls

MNI coordinates			Area	Cluster sizes	Z-score	P-value*
x	y	z				
−14	−4	22	Left caudate	139	4.53	0.002
14	−4	22	Right caudate	130	4.01	0.004
−28	−8	12	Left putamen	519	4.28	0.006
28	−8	12	Right putamen	420	3.83	0.028
22	−6	2	Left globus pallidus	74	2.90	0.031
−22	−6	2	Right globus pallidus	46	2.71	0.038

*P-values are FWE corrected except for globus pallidus where P-values are uncorrected.

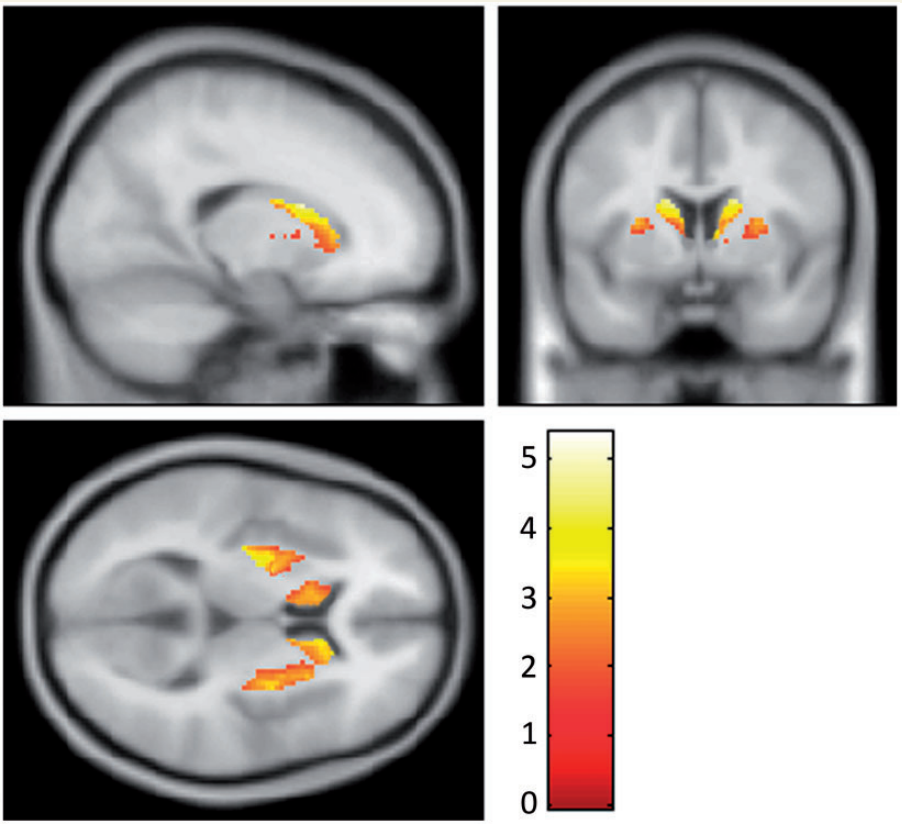

Figure 2 Statistical parametric maps of ^{11}C-IMA107 BP_{ND} (MNI co-ordinates x = 17.99, y = 3.59, z = 7.42). Yellow–red areas represent voxel clusters with significant decreases in ^{11}C-IMA107 BP_{ND} within the basal ganglia mask in Parkinson's disease patients. The colour stripe indicates z-values.

Our findings raise the possibility that, as with dopaminergic acting drugs such as levodopa and dopamine agonists, PDE10A modulating drugs may have a therapeutic role in Parkinson's disease. Similar to previous studies with dopaminergic markers, PDE10A loss did not correlate with tremor, which may be explicable by tremor pathophysiology being more closely related to serotonergic deficits (Loane *et al.*, 2013).

Axial signs such as imbalance, falls and freezing of gait are not associated with the degree of nigrostriatal dopaminergic denervation and they are often refractory to treatment with dopaminergic medication (Bohnen *et al.*, 2009). In our study, we found that worse axial signs were associated with loss of PDE10A in globus pallidus. Deep brain stimulation of the globus pallidus has been shown to have variable effects on gait and balance problems in Parkinson's disease (Krack *et al.*, 1998; Pötter-Nerger and Volkmann, 2013), and can even provoke gait freezing in patients with cervical dystonia (Berman *et al.*, 2009). Moreover, recent functional MRI studies have demonstrated that freezing of gait is associated with decreased blood oxygen level-dependent signal in the globus pallidus during a virtual reality gait task (Shine *et al.*, 2013; Peterson *et al.*, 2014). We speculate that loss of PDE10A in the globus pallidus

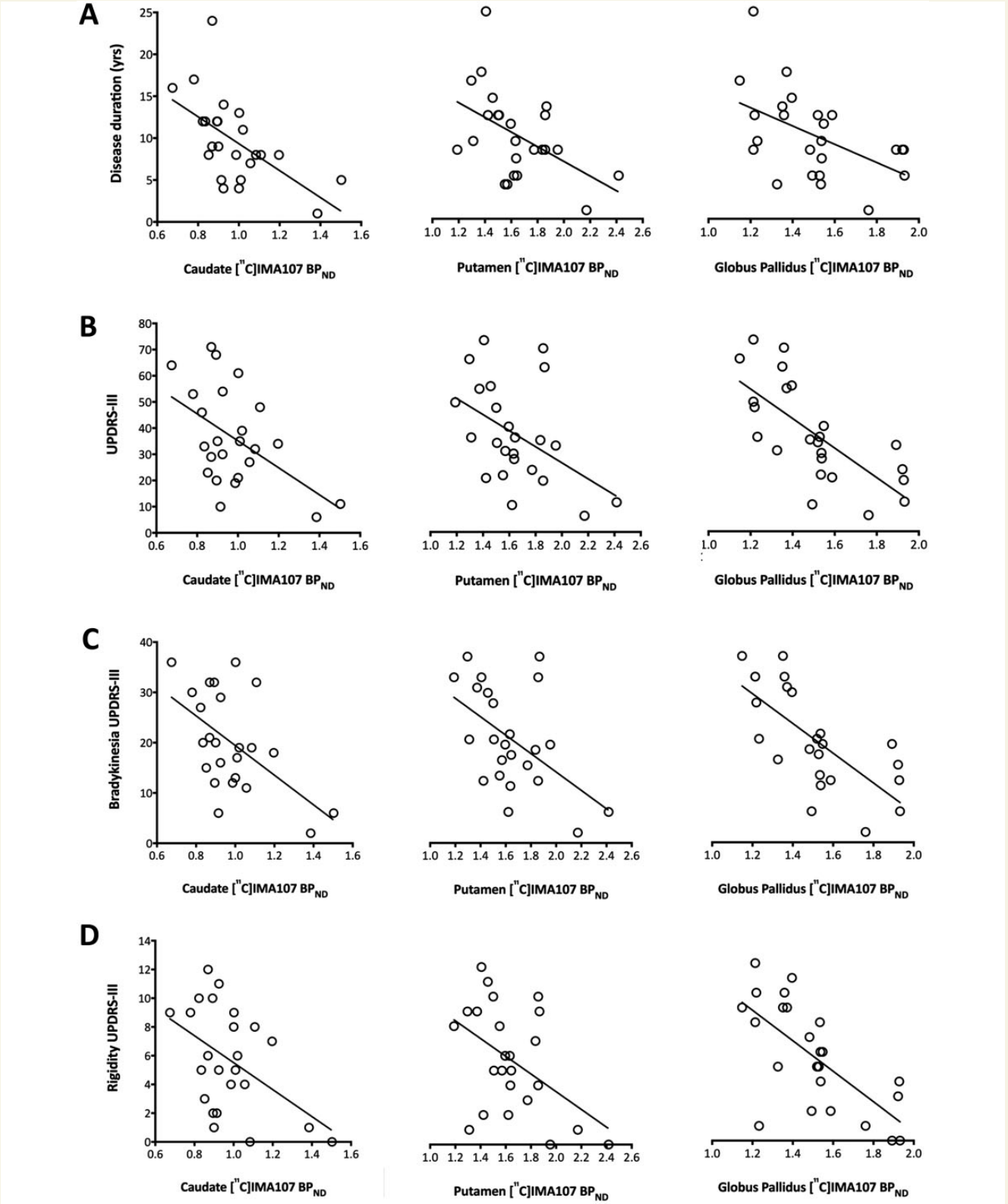

Figure 3 Correlations between loss of PDE10A and progression and severity of Parkinson's disease. (**A**) Longer disease duration correlated with lower ^{11}C-IMA107 BP_{ND} in caudate ($r = -0.65$; $P = 0.005$), putamen ($r = -0.51$; $P = 0.025$) and globus pallidus ($r = -0.47$; $P = 0.03$). (**B**) Higher UPDRS-III scores correlated with lower ^{11}C-IMA107 BP_{ND} ratio in caudate ($r = -0.54$; $P = 0.011$), putamen ($r = -0.48$; $P = 0.022$) and globus pallidus ($r = -0.70$; $P < 0.001$). (**C**) Higher bradykinesia subscore was correlated with lower ^{11}C-IMA107 BP_{ND} in caudate ($r = -0.58$; $P = 0.007$), putamen ($r = -0.53$; $P = 0.010$) and globus pallidus ($r = -0.69$; $P < 0.001$). (**D**) Higher rigidity subscore was correlated with lower ^{11}C-IMA107 BP_{ND} in caudate ($r = -0.51$; $P = 0.022$), putamen ($r = -0.48$; $P = 0.022$) and globus pallidus ($r = -0.67$; $P < 0.001$).

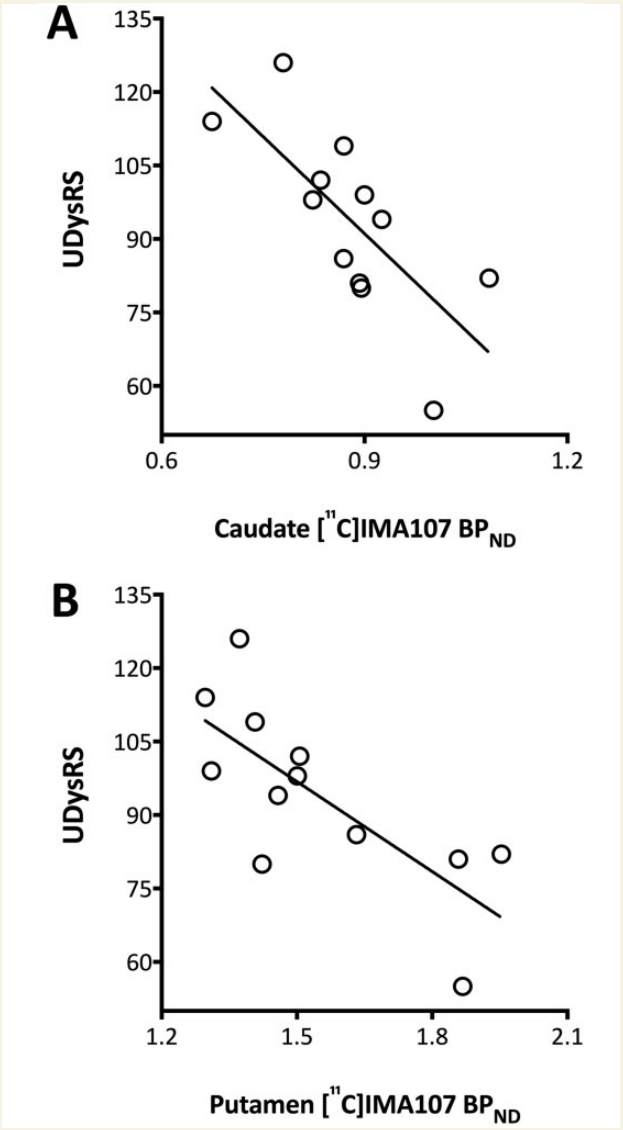

Figure 4 Correlations between loss of PDE10A and severity of levodopa-induced dyskinesias in 12 Parkinson's disease patients with motor complications. Higher UDysRS scores correlated with lower ^{11}C-IMA107 BP_{ND} in (**A**) caudate ($r = -0.73$, $P = 0.031$) and (**B**) putamen ($r = -0.74$, $P = 0.031$).

may contribute to the development of axial signs in Parkinson's disease.

Dopaminergic signalling is regulated by PDE10A through the cAMP/PKA/DARPP-32 signalling cascade (Greengard *et al.*, 1999; Nishi *et al.*, 2008; Girault, 2012). PDE10A has different roles in modulating cAMP signalling in the striato-nigral and striato-pallidial postsynaptic pathways. In striato-nigral neurons, dopamine loss leads to a reduced synthesis of D1 receptor-stimulated cAMP (Herve *et al.*, 2001); decreased PDE10A expression will therefore increase cAMP levels and could in part compensate for the reduced cAMP signalling. In striato-pallidal neurons, dopamine loss decreases the inhibitory effect of D2 receptor on cAMP synthesis (Stoof and Kebabian, 1981). Decreased PDE10A levels may further increase cAMP levels by enhancing the negative consequences of dopamine loss on D2 receptor signalling and potentiate adenosine A2A receptor signalling. Hence, loss of PDE10A may result in functional imbalance between the striato-nigral and striato-pallidal dopaminergic pathways depressing motor activity and contributing to the development of Parkinson's disease symptoms.

Half of our patients with Parkinson's disease had more advanced disease and were exhibiting LIDs. In Parkinson's disease patients with LIDs, region of interest-based analysis of PET signalling showed 19–34% reductions in PDE10A expression in the caudate, substantia nigra and motor thalamic nuclei, compared to Parkinson's disease patients with stable response to levodopa. These significant changes in the Parkinson's disease LIDs subgroup were not confirmed at a voxel level and did not survive after using disease duration as a covariate in the analysis. These observations raise the possibility that further PDE10A decreases in Parkinson's disease patients with LIDs are the result of advanced disease rather directly related to the development of LIDs. However, when we assessed dyskinesia severity, rather than simply dyskinesia presence/absence, worse LIDs scores independently correlated with loss of striatal PDE10A expression. It is unclear at this stage whether PDE10A has a direct relevance to the development of LIDs in Parkinson's disease, or whether this is simply an epiphenomenon. The prevalence of LIDs increases and PDE10 expression decreases with advancing Parkinson's disease, but a study comparing PDE10A expression between Parkinson's disease patients, matched for disease duration, with and without LIDs would be able to answer this question.

Preclinical studies have suggested that PDE10A could be involved in the development of Parkinson's disease LIDs. In dyskinetic Parkinson's disease rats, striatal second messenger signalling was altered at the peak of dyskinesias due to the lost ability of striatal medium spiny neurons to induce both long-term potentiation and long-term depression (Picconi *et al.*, 2003, 2008, 2011). This means that stimulation of postsynaptic striatal neurons from levodopa-derived dopamine would fail and dysregulation of PDE10A could be a pathogenic mechanism underlying the dysfunction of second messenger signalling. In dyskinetic rodent models of Parkinson's disease, cAMP levels in the cortico-striatal-pallidal pathway were significantly reduced at peak of dyskinesias compared to non-dyskinetic animals, and administration of the non-selective phosphodiesterase inhibitor, zaprinast, before levodopa effectively reduced the severity of dyskinesias and prevented the decreases in cyclic nucleotides levels (Giorgi *et al.*, 2008). A recent study has shown lower striatal cAMP and cGMP levels in dyskinetic animals at 60 min after levodopa administration (Sancesario *et al.*, 2014). During the phase of decreasing and extinction of dyskinesias (from 90 to 150 min after levodopa), cAMP/cGMP levels were upregulated in dyskinetic animals. Thus, changes in cyclic nucleotide levels are

linked to the appearance and regression of LIDs. Cyclic nucleotides levels are regulated by both dopamine-induced synthesis and PDE-related catabolism. It has been previously demonstrated that LIDs are associated with short-term sharp rises in synaptic dopamine levels following levodopa administration (de la Fuente-Fernandez *et al.*, 2001; Politis *et al.*, 2014). Hence, altered cyclic nucleotides levels due to abnormal dopamine-induced synthesis and PDE10A-related catabolism might contribute to the development of LIDs.

Recent PET studies have demonstrated the importance of PDE10A in other movement disorders such as Huntington's disease (Ahmad *et al.*, 2014; Russell *et al.*, 2014). Striatal PDE10A levels were decreased by 48–70% in manifest Huntington's disease gene carriers (Ahmad *et al.*, 2014; Russell *et al.*, 2014). Similar to what was observed in our cohort of Parkinson's disease patients, loss of striatal PDE10A expression correlated with worse Unified Huntington's Disease Rating Scale–Motor scores in manifest Huntington's disease gene carriers (Russell *et al.*, 2014). Collectively, these observations suggest an extended role for the importance of PDE10A expression in the clinical presentation of movement disorders.

In conclusion, our findings provide evidence for a novel neurochemical change in Parkinson's disease, which is linked with the progression and severity of motor symptoms. ^{11}C-IMA107 PET may be a valuable tool to understand the pathophysiology of Parkinson's disease. PDE10A could serve as a novel therapeutic target for manipulation with pharmacotherapy, and PDE10A modulating drugs by acting independently or synergistically with levodopa could potentially have a therapeutic role in the alleviation of Parkinson's disease symptoms and complications.

Acknowledgements

We thank all participants and their families, the PET technicians and radiochemists, the MRI radiographers, and the clinical research nurses at Imanova Ltd for their cooperation and support with this study. Flavia Niccolini is supported from Parkinson's UK. Tom Foltynie's research is supported by the Brain Research Trust, UCL's NIHR Biomedical Research Unit, the European Union FP-7 scheme and the Michael J. Fox Foundation. Marios Politis research is supported by Parkinson's UK, Lily and Edmond J. Safra Foundation, Michael J Fox Foundation (MJFF) for Parkinson's research, and KCL's NIHR Biomedical Research Unit.

Funding

This research was supported by Parkinson's UK. This research was also part supported by the National Institute for Health Research (NIHR) Mental Health Biomedical Research Centre at South London and Maudsley NHS Foundation. The views expressed are those of the authors and not necessarily those of the NHS, the NIHR or the Department of Health.

Supplementary material

Supplementary material is available at *Brain* online.

References

Ahmad R, Bourgeois S, Postnov A, Schmidt ME, Bormans G, Van Laere K, et al. PET imaging shows loss of striatal PDE10A in patients with Huntington disease. Neurology 2014; 82: 279–81.

Ashburner J, Friston KJ. Nonlinear spatial normalization using basis functions. Hum Brain Mapp 1999; 7: 254–66.

Barret O, Thomae D, Tavares A, Alagille D, Papin C, Waterhouse R, et al. *In vivo* assessment and dosimetry of 2 novel PDE10A PET radiotracers in humans: 18F-MNI-659 and 18F-MNI-654. J Nucleic Med 2014; 55: 1297–304.

Benjamini Y, Hochberg Y. Controlling the false discovery rate: a practical and powerful approach to multiple testing. J R Stat Soc Series B Stat Methodol 1995; 57: 289–300.

Berman BD, Starr PA, Marks WJ, Jr, Ostrem JL. Induction of bradykinesia with pallidal deep brain stimulation in patients with cranial-cervical dystonia. Stereotact Funct Neurosurg 2009; 87: 37–44.

Bohnen NI, Müller ML, Koeppe RA, Studenski SA, Kilbourn MA, Frey KA, et al. History of falls in Parkinson disease is associated with reduced cholinergic activity. Neurology 2009; 73: 1670–6.

Booij J, Tissingh G, Boer GJ, Speelman JD, Stoof JC, Janssen AG, et al. [123I]FP-CIT SPECT shows a pronounced decline of striatal dopamine transporter labelling in early and advanced Parkinson's disease. J Neurol Neurosurg Psychiatry 1997; 62: 133–40.

Broussolle E, Dentresangle C, Landais P, Garcia-Larrea L, Pollak P, Croisile B, et al. The relation of putamen and caudate nucleus ^{18}F-Dopa uptake to motor and cognitive performances in Parkinson's disease. J Neurol Sci 1999; 166: 141–51.

Buckner RL, Head D, Parker J, Fotenos AF, Marcus D, Morris JC, et al. A unified approach for morphometric and functional data analysis in young, old, and demented adults using automated atlas-based head size normalization: reliability and validation against manual measurement of total intracranial volume. Neuroimage 2004; 23: 724–38.

Coskran TM, Morton D, Menniti FS, Adamowicz WO, Kleiman RJ, Ryan AM, et al. Immunohistochemical localization of phosphodiesterase 10A in multiple mammalian species. J Histochem Cytochem 2006; 54: 1205–13.

Cotzias GC, Papavasiliou PS, Gellene R. Modification of Parkinsonism: chronic treatment with L-dopa. N Engl J Med 1969; 280: 337–45.

Cotzias GC, Van Woert MH, Schiffer LM. Aromatic amino acids and modification of parkinsonism. N Engl J Med 1967; 276: 374–9.

de la Fuente-Fernandez R, Lu JQ, Sossi V, Jivan S, Schulzer M, Holden JE, Lee CS, et al. Biochemical variations in the synaptic levels of dopamine precede motor fluctuations in Parkinson's disease: PET evidence of increased dopamine turnover. Ann Neurol 2001; 49: 298–303.

Fischl B, Salat DH, Busa E, Albert M, Dieterich M, Haselgrove C, et al. Whole Brain Segmentation: Automated Labeling of Neuroanatomical Structures in the Human Brain. Neuron 2002; 33: 341–55.

Fredholm BB, Bättig K, Holmén J, Nehlig A, Zvartau EE. Actions of caffeine in the brain with special reference to factors that contribute to its widespread use. Pharmacol Rev 1999; 51: 83–133.

Friston KJ, Holmes AP, Worsley KJ, Poline JB, Frith CD, Frackowiak RS. Statistical parametric maps in functional imaging: a general linear approach. Hum Brain Mapp 1995; 2: 189–210.

Fujishige K, Kotera J, Omori K. Striatum- and testis-specific phosphodiesterase PDE10A isolation and characterization of a rat PDE10A. Eur J Biochem 1999; 266: 1118–27.

Giorgi M, D'Angelo V, Esposito Z, Nuccetelli V, Sorge R, Martorana A, et al. Lowered cAMP and cGMP signalling in the brain during levodopa-induced dyskinesias in hemiparkinsonian rats: new aspects in the pathogenetic mechanisms. Eur J Neurosci 2008; 28: 941–50.

Giorgi M, Melchiorri G, Nuccetelli V, D'Angelo V, Martorana A, Sorge R, et al. PDE10A and PDE10A-dependent cAMP catabolism are dysregulated oppositely in striatum and nucleus accumbens after lesion of midbrain dopamine neurons in rat: a key step in parkinsonism physiopathology. Neurobiol Dis 2011; 43: 293–303.

Girault JA. Integrating neurotransmission in striatal medium spiny neurons. Adv Exp Med Biol 2012; 970: 407–29.

Greengard P, Allen PB, Nairn AC. Beyond the dopamine receptor: the DARPP- 32/protein phosphatase-1 cascade. Neuron 1999; 23: 435–47.

Gunn RN, Lammertsma AA, Hume SP, Cunningham VJ. Parametric imaging of ligand-receptor binding in PET using a simplified reference region model. Neuroimage 1997; 6: 279–87.

Herve D, Le Moine C, Corvol JC, Belluscio L, Ledent C, Fienberg AA, et al. Galpha(olf) levels are regulated by receptor usage and control dopamine and adenosine action in the striatum. J Neurosci 2001; 21: 4390–99.

Hossain MA, Weiner N. Dopaminergic functional supersensitivity: effects of chronic L-dopa and carbidopa treatment in an animal model of Parkinson's disease. J Pharmacol Exp Ther 1993; 267: 1105–11.

Hsiao IT, Weng YH, Hsieh CJ, Lin WY, Wey SP, Kung MP, et al. Correlation of Parkinson disease severity and 18F-DTBZ positron emission tomography. JAMA Neurol 2014; 71: 758–66.

Jellinger KA. Pathology of Parkinson's disease. Mol Chem Neuropathol 1991; 3: 153–97.

Kelly MP, Adamowicz W, Bove S, Hartman AJ, Mariga A, Pathak G, et al. Select 3',5'-cyclic nucleotide phosphodiesterases exhibit altered expression in the aged rodent brain. Cell Signal 2014; 26: 383–97.

Krack P, Pollak P, Limousin P, Hoffmann D, Xie J, Benazzouz A, et al. Subthalamic nucleus or internal pallidal stimulation in young onset Parkinson's disease. Brain 1998; 121: 451–7.

Lees AJ, Shaw KM, Stern GM. "Off period" dystonia and "on period" choreoathetosis in levodopatreated patients with Parkinson's disease. Lancet 1977; 2: 1034.

Loane C, Wu K, Bain P, Brooks DJ, Piccini P, Politis M. Serotonergic loss in motor circuitries correlates with severity of action-postural tremor in PD. Neurology 2013; 80: 1850–5.

Marek K, Innis R, van Dyck C, Fussell B, Early M, Eberly S, et al. [^{123}I]beta-CIT SPECT imaging assessment of the rate of Parkinson's disease progression. Neurology 2001; 57: 2089–94.

Montgomery AJ, Thielemans K, Mehta MA, Turkheimer F, Mustafovic S, Grasby PM. Correction of head movement on PET studies: comparison of methods. J Nucleic Med 2006; 47: 1936–44.

Nishi A, Kuroiwa M, Miller DB, O'Callaghan JP, Bateup HS, Shuto T, et al. Distinct roles of PDE4 and PDE10A in the regulation of cAMP/PKA signaling in the striatum. J Neurosci 2008; 28: 10460–71.

Otsuka M, Ichiya Y, Kuwabara Y, Hosokawa S, Sasaki M, Yoshida T, et al. Differences in the reduced ^{18}F-Dopa uptakes of the caudate and the putamen in Parkinson's disease: correlations with the three main symptoms. J Neurol Sci 1996; 136: 169–73.

Peterson DS, Pickett KA, Duncan RP, Perlmutter JS, Earhart GM. Brain activity during complex imagined gait tasks in Parkinson disease. Clin Neurophysiol 2014; 125: 995–1005.

Picconi B, Bagetta V, Ghiglieri V, Paillè V, Greengard P, Fisone G, et al. Inhibition of phosphodiesterases rescues striatal long-term depression and reduces levodopa-induced dyskinesia. Brain 2011; 134: 375–87.

Picconi B, Centonze D, Håkansson K, Bernardi G, Barone I, Lindgren HS, et al. Loss of bidirectional striatal synaptic plasticity in L-DOPA-induced dyskinesia. Nat Neurosci 2003; 6: 501–6.

Picconi B, Paillé V, Ghiglieri V, Bagetta V, Di Filippo M, Pendolino V, et al. l-DOPA dosage is critically involved in dyskinesia via loss of synaptic depotentiation. Neurobiol Dis 2008; 229: 327–35.

Plisson C, Salinas C, Weinzimmer D, Labaree D, Lin SF, Ding YS, et al. Radiosynthesis and *in vivo* evaluation of [(11)C]MP-10 as a positron emission tomography radioligand for phosphodiesterase 10A. Nucleic Med Biol 2011; 38: 875–84.

Plisson C, Weinzimmer D, Jakobsen S, Natesan S, Salinas C, Lin SF, et al. Phosphodiesterase 10A PET radioligand development program: from pig to human. J Nucleic Med 2014; 55: 595–601.

Politis M, Wu K, Loane C, Kiferle L, Molloy S, Brooks DJ, et al. P, Staging of serotonergic dysfunction in Parkinson's disease: an in vivo 11C-DASB PET study. Neurobiol Dis 2010; 40: 216–21.

Politis M, Wu K, Loane C, Brooks DJ, Kiferle L, Turkheimer FE, et al. Serotonergic mechanisms responsible for levodopa-induced dyskinesias in Parkinson's disease patients. J Clin Invest 2014; 124: 1340–9.

Pötter-Nerger M, Volkmann J. Deep brain stimulation for gait and postural symptoms in Parkinson's disease. Mov Disord 2013; 28: 1609–15.

Prodoehl J, Yu H, Little DM, Abraham I, Vaillancourt DE. Region of interest template for the human basal ganglia: comparing EPI and standardized space approaches. Neuroimage 2008; 39: 956–65.

Rasmussen H. Cell communication, calcium ion, and cyclic adenosine monophosphate. Science 1970; 170: 404–12.

Russell DS, Barret O, Jennings DL, Friedman JH, Tamagnan GD, Thomae D, et al. The phosphodiesterase 10 positron emission tomography tracer, [18F]MNI-659, as a novel biomarker for early huntington disease. JAMA Neurol 2014; 71: 1520–8.

Sancesario G, Morrone LA, D'Angelo V, Castelli V, Ferrazzoli D, Sica F, et al. Levodopa-induced dyskinesias are associated with transient down-regulation of cAMP and cGMP in the caudate-putamen of hemiparkinsonian rats: reduced synthesis or increased catabolism? Neurochem Int 2014; 79: 44–56.

Seeger TF, Bartlett B, Coskran TM, Culp JS, James LC, Krull DL, et al. Immunohistochemical localization of PDE10A in the rat brain. Brain Res 2003; 985: 113–126.

Shine JM, Matar E, Ward PB, Bolitho SJ, Gilat M, Pearson M, et al. Exploring the cortical and subcortical functional magnetic resonance imaging changes associated with freezing in Parkinson's disease. Brain 2013; 136: 1204–15.

Stoof JC, Kebabian JW. Opposing roles for D-1 and D-2 dopamine receptors in efflux of cyclic AMP from rat neostriatum. Nature 1981; 294: 366–8.

Studholme C, Hill DL, Hawkes DJ. Automated three-dimensional registration of magnetic resonance and positron emission tomography brain images by multiresolution optimization of voxel similarity measures. Med Phys 1997; 24: 25–35.

Sudhyadhom A, Haq IU, Foote KD, Okun MS, Bova FJ. A high resolution and high contrast MRI for differentiation of subcortical structures for DBS targeting: The Fast Gray Matter Acquisition T1 Inversion Recovery (FGATIR), Neuroimage 2009; 47: T44–52.

Tanner M, Gambarota G, Kober T, Krueger G, Erritzoe D, Marques JP, et al. Fluid and white matter suppression with the MP2RAGE sequence. J Magn Reson Imaging 2013; 35: 1063–70.

Tenn CC, Niles LP. Sensitization of G protein-coupled benzodiazepine receptors in the striatum of 6-hydroxydopamine-lesioned rats. J Neurochem 1997; 69: 1920–6.

Tziortzi AC, Searle GE, Tzimopoulou S, Salinas C, Beaver JD, Jenkinson M, et al. Imaging dopamine receptors in humans with [11C]-(+)-PHNO: dissection of D3 signal and anatomy. Neuroimage 2011; 54: 264–77.